Structural Defects and Acidic and Basic Sites in Sol−Gel MgO

J. A. Wang, O. Novaro,*,† and X. Bokhimi

Institute of Physics, The National University of Mexico (UNAM), A. P. 20-364, 01000 México D. F., Mexico

T. López and R. Gómez

Departamento de Química, Universidad Autónama Metropolitana-Iztapalapa, A. P. 55-534, 09340 México D. F., Mexico

J. Navarrete, M. E. Llanos, and E. López-Salinas

Instituto Mexicano del Petróleo, Eje Central Lázaro Cárdenas 125, 07730 México D. F., Mexico

Received: January 16, 1997; In Final Form: May 27, 1997[⊗]

MgO prepared with the sol−gel technique had crystalline structure defects, obtained from X-ray powder diffraction and crystalline structure refinement, that correlated with its acidic and basic sites. The acidic sites, measured by adsorbing pyridine and NH_3, were found when brucite and MgO coexisted, which only occurred after annealing the sample at 673 K. Two different basic sites, measured by adsorbing CO_2, were present in a total concentration of about 10^{21} sites per gram. These sites correlated to the presence of magnesium vacancies in MgO crystal. Both basic site and magnesium vacancy concentrations diminished when the sample annealing temperature was increased.

Introduction

Surface properties of catalysts, especially surface acidity and basicity, are important in acid−base catalyzed reactions.[1−7] The formation of the corresponding acid and basic sites can significantly be affected by defects in the catalyst crystalline structure.[8,9] The type of defect can be controlled by doping the material, and the defect number, by controlling the specific surface area.

One of the methods for producing materials with a large amount of defects is the sol−gel technique, which has been widely applied during the past 15 years for preparing catalysts, catalyst supports, and ceramic composites.[10−13] Inherent to the sol−gel technique is the presence of OH ions that in many cases determine the final product and in some others go into the crystalline structure generating defects, as observed in sol−gel MgO,[14] which is a material of interest in catalysis.

MgO (periclase) as a solid catalyst or catalyst support is attractive for heterogeneous catalytic reactions like Aldol condensation.[15,16] MgO is also used as a catalyst support because it improves the selectivity and stabilizes the active metal in unusual electronic states, for example, in Pt/MgO,[17] Ru−Cu/MgO,[18] and Pt−Ru/MgO[19] catalysts.

Nowadays, most MgO is prepared by using conventional methods based on the decomposition of various magnesium salts and $Mg(OH)_2$ (brucite).[20−24] More than 75% MgO is produced from brucite.[25] Therefore, the decomposition mechanism of brucite to form MgO has been extensively studied,[26,27] generating different models that compare brucite and periclase crystalline structures.[28−30] The MgO prepared by conventional methods, however, often yields a relatively small surface area, which for some applications is a disadvantage.

This disadvantage is eliminated when MgO is prepared by using the sol−gel technique.[31] Catalysts prepared with this technique exhibit smaller particle size, larger specific surface area, higher purity, and a large number of defects in the crystalline structure; these parameters usually play an important role in catalytic reactions.

As mentioned above, defects on crystals surface promote the formation of basic and acid sites. Klabunde et al. used phosphate compounds as a molecular probe to study the decomposition reactions of a set of phosphate compounds on MgO, finding that surface defects sites were involved in this decomposition.[32−36] This differs from the results of Ohmacht and Nobutsune et al., who found that oxygen and magnesium in MgO lattice sites are responsible for the activity of ethanol and 2-propanol decomposition reactions.[37,38] Therefore, a study of the relationship between surface acidic and basic sites and defects in the crystalline structure of sol−gel MgO will be of interest and will help to understand the mechanism on some catalytic reactions involving MgO.

In this paper, we will report the formation of basic and acid sites in MgO prepared with the sol−gel technique and their relation to crystalline structure defects. The analysis was done with X-ray powder diffraction together with refinement of the crystalline structure, infrared spectroscopy of pyridine desorption, and thermal desorption of NH_3 and CO_2.

Experimental Section

Catalyst Preparation. Samples were synthesized at pH 5 with $Mg(OC_2H_5)_2$ and $H_2C_2O_4$ (oxalic acid) as hydrolysis catalyst. More details about sample preparation can be found elsewhere.[39] Before characterization, samples were annealed in air at indicated temperature for 8 h.

Catalyst Characterization. X-ray powder diffraction analysis was performed at room temperature on a Siemens D-5000 diffractometer with Cu Kα radiation. Intensities were measured in the 2θ range between 10° and 110°, with a 2θ step of 0.02° and a measuring time of 1.03 s per point. Periclase and brucite crystalline structures were refined with the Rietveld method. From the refinement, average crystallite size and magnesium vacancy were also obtained.

† Member of El Colegio Nacional, Mexico.

* To whom correspondence should be addressed. Phone (52)5 6161535; Fax (52)5 6161535; E-mail novaro@fenix.ifisicacu.unam.mx.

⊗ Abstract published in *Advance ACS Abstracts,* September 1, 1997.

S1089-5647(97)00233-2 CCC: $14.00

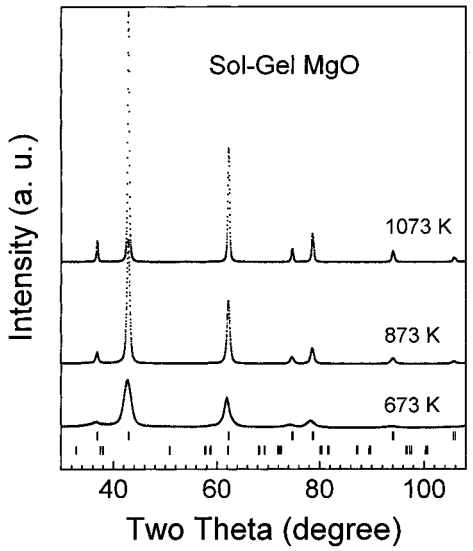

Figure 1. X-ray diffraction patterns after annealing the sample at different temperatures. Upper tick marks correspond to periclase and lower tick marks to brucite.

Samples were characterized with a 170-SX Fourier transform infrared (FTIR) spectrometer. Before pyridine adsorption, the sample in a vacuum was heated to 673 K at a rate of 20 K/min and cooled to room temperature. It was then exposed for 20 min to pyridine by breaking, in the spectrometer cell, a capillary tube containing 100 μL of pyridine. Thereafter, its infrared spectrum was recorded while outgassing at the temperature of interest.

Total basicity of the sample was measured by thermal desorption of CO_2 and the total acidity by thermal desorption of NH_3. Before these measurements, the samples in flowing He were pretreated for 30 min at 737 K to desorb impurities. After that, CO_2 (NH_3) was introduced into the sample bed at room temperature and maintained there for 30 min. Nonadsorbed CO_2 (NH_3) was eliminated by flowing He on the sample. Finally, sample desorption occurred by heating it at 10 K/min.

Results and Discussion

Crystalline Structure Analysis. Sol−gel MgO prepared with different hydrolysis catalysts has it smallest average crystallite size when oxalic acid is the hydrolysis catalyst.[39] This size correlated with the magnesium deficiency in the crystalline structure. Hence, for the present study this acid was used as hydrolysis catalyst for preparing the sol−gel MgO samples.

Figure 1 shows the X-ray diffraction patterns after annealing the sample at 673, 873, and 1073 K. The sample annealed at 673 K had brucite (6.2 wt %) and periclase (93.8 wt %). When the annealing temperature was increased, the diffraction peaks of MgO become narrower, because the average crystallite size also increased.

Periclase crystalline structure was refined with the unit cell described by Bokhimi et al.[39] and brucite crystalline structure with a hexagonal unit cell with space group *P*-3*m1*. Because of their importance for the present work, special attention was paid to the defects in the crystalline lattice. Figure 2 shows a typical refinement plot for the sample annealed at 873 K.

After annealing the sample from 673 to 1073 K, the MgO lattice parameter decreased from 0.422 94(6) to 0.421 45(5) nm, and its average crystallite size increased from 21.2(4) to 23.7-(2) nm (Table 1). The Mg:O atomic ratio was less than 1.0, the stoichiometric value, because MgO crystalline structure was deficient in magnesium (Table 1). The defect concentration of this cation decreased from 8.17% at 673 K to 6.90% at 1073 K. Generally, cations reach their stable positions through the oxygen framework by diffusion or migration, which increases with the annealing temperature. This explains why the number of magnesium defects reduced by increasing the annealing temperature.

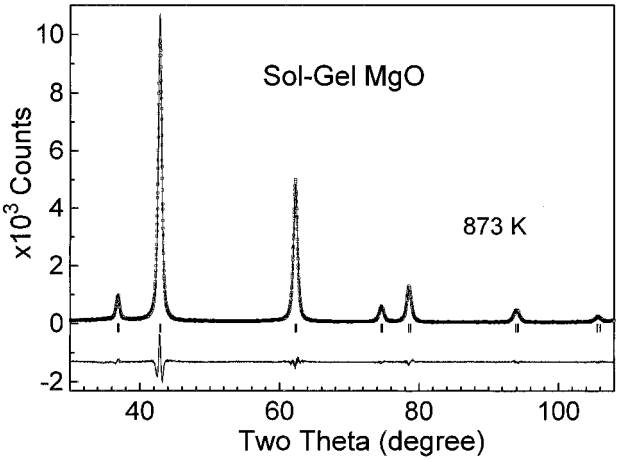

Figure 2. Rietveld refinement plot of sol−gel MgO annealed at 873 K. $R_{wp} = 0.079$. Tick marks correspond to periclase.

TABLE 1: MgO Lattice Parameters, Average Crystalline Size, and Magnesium Vacancy Concentration as a Function of Sample Annealing Temperature

annealing temp (K)	673	873	1073
lattice parameters[a] (nm)	0.42294(6)	0.42146(1)	0.42145(5)
av crystalline size[a] (nm)	21.2(4)	23.4(2)	23.7(2)
Mg vacancy concn (%)	8.17	7.21	6.90
no. of Mg vacancies per unit cell	0.33	0.29	0.27

[a] Estimated standard deviations, obtained from the refinement, are shown in parentheses.

The formation mechanism responsible for the magnesium deficiency relates to the residual OH^- groups in the MgO lattice. The rearrangement of atoms in the crystalline structure of [Mg−O···H−H···O−Mg] results in the formation of cation deficiency on the surface or in the bulk of the crystal (or in both).[14]

Acidic and Basic Sites Analysis. The FTIR spectra of pyridine, adsorbed on the sample annealed at 673 K, had two absorption bands that are characteristic of surface Lewis acid sites:[40] one at 1445 cm^{-1} and another at 1487 cm^{-1} (Figure 3). The interaction that generated the band at 1445 cm^{-1} was so weak that at room temperature the band rapidly disappeared during outgassing; the interaction associated with the band at 1487 cm^{-1}, however, was more temperature stable.

Acid sites were also measured by adsorbing NH_3. The sample annealed at 673 K adsorbed only 134 μmol/g of NH_3 on its surface, confirming the observed weak acidity. When the sample was annealed at 873 and 1073 K, no more NH_3 adsorption was observed because the acid sites disappeared.

As it was mentioned in the crystalline structure analysis, the main difference between the samples annealed at different temperatures was that the one annealed at 673 K had 6.2 wt % brucite. Moreover, this was the only sample that had acidic sites. Therefore, these acidic sites can be related to the presence of this crystalline phase, which during dehydroxylation was transformed into periclase, generating vacancies in the lattice. During this brucite transformation, water was formed from two OH ions that on a local scale were substituted for one oxygen ion and one anion vacancy (Scheme 1). When the sample was annealed at a higher temperature, the dehydroxylation continued, forming increasingly anion vacancies until the structure col-

TABLE 2: CO_2 Adsorption Data as a Function of Sample Annealing Temperature[a]

	peak I			peak II			total	
annealing temp (K)	W (μmol/g)	N (10^{20}/g)	T_{max} (K)	W (μmol/g)	N (10^{20}/g)	T_{max} (K)	W (μmol/g)	N (10^{20}/g)
673	727	4.41	398	671	4.27	493	1398	8.68
873	555	3.34	398	627	3.78	493	1182	7.12
1073	402	2.50	372	512	3.19	483	914	5.69

[a] W = amount of adsorbed CO_2, N = number of basic sites, and T_{max} = the temperature at which CO_2 desorption rate achieved its maximum.

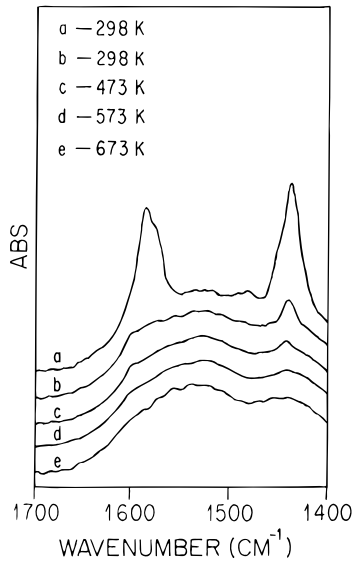

Figure 3. FTIR spectra of the samples with adsorbed pyridine at various temperatures. It was taken while outgassing the sample in a vacuum.

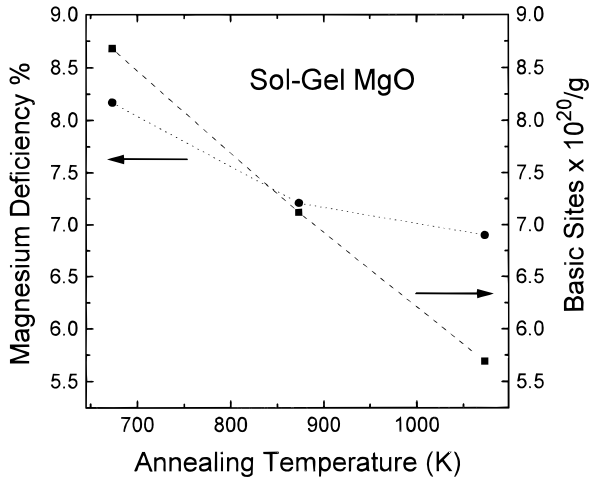

Figure 4. Magnesium vacancy and basic site concentrations as a function of the sample annealing temperature.

SCHEME 1: One Oxygen Vacancy Site (□) Was Created during the Transformation from Brucite to MgO

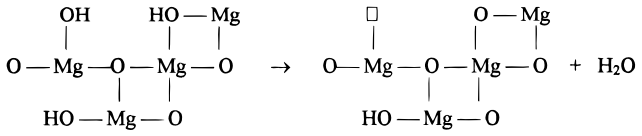

lapsed into MgO crystalline structure, which caused the anion vacancies generated during brucite transformation to disappear.

The anion vacancies described above could be responsible for the observed acidic behavior of the sample annealed at 673 K. If there was an anion vacancy in the structure, some magnesium ions should be around this site, locally producing a positive charge. In this model, nitrogen atoms, which have two rich electrons in the NH_3 molecule, were adsorbed on this site, balancing the extra positive charge.

Using CO_2 adsorption identified basic sites. The total amount of adsorbed carbon dioxide molecules depended on the sample annealing temperature (Table 2). The sample annealed at 673 K had the largest number of total basic sites: -8.86×10^{20} basic sites per gram. When the sample was annealed from 873 to 1073 K, the number of basic centers reduced from 7.12×10^{20} to 5.69×10^{20} sites per gram.

Basic sites had a close relation to specific surface area, crystallite size, and crystalline structure defects. After annealing samples at 673 K, MgO crystals had an average size of 21.2(4) nm and many magnesium vacancies (Table 1). This explains the observed huge number of basic centers at this temperature. After annealing the sample at a higher temperature, the average crystallite size increased, and the number of Mg vacancies decreased. Accordingly, the number of basic sites diminished (Table 2).

For all annealing temperatures, samples had two CO_2 desorption peaks associated with two different basic sites. When this temperature increased, the area of these peaks, which was associated with the number of basic sites, changed differently: the number of the weak basic sites decreased faster than the number of the strong basic sites (Table 2).

The strength of the observed basic sites depended on sample annealing temperature. When this temperature increased from 673 to 873 K, the temperature at the maximum rate of CO_2 desorption, T_{max}, of both peak I and peak II did not change. When the sample was heated at 1073 K, however, T_{max} shifted from 398 to 372 K for peak I and from 493 to 483 K for peak II, indicating a diminishing of the basicity strength. These observed changes of the basic site concentration and the basicity strength with annealing temperature had an effect on the activity of the MgO samples in the acid−base catalyzed reaction.[41]

Both magnesium vacancies and basic sites decreased when annealing temperature was increased (Figure 4); the basic site concentration decreased almost linearly with temperature. The variation of magnesium vacancy concentration with temperature, however, was not linear, but it followed the same tendency with temperature as the basic site concentration. The observed different temperature dependence between magnesium vacancies and basic sites suggests that not all acid sites were associated with magnesium vacancies.

Conclusions

Brucite mixed with MgO, which occurred after annealing the sample at 673 K, produced Lewis acid sites that disappeared after annealing the sample at higher temperatures. The presence of these sites was explained with a model based on anion vacancies produced during the transformation of brucite into MgO.

MgO crystalline structure had cation vacancies that produced two basic sites with different strengths. The total concentration of basic sites was about 10^{21} sites per gram and decreased when the annealing temperature of the sample was increased.

The high basicity of the sol−gel MgO will be of great interest for those involved in basic catalytic reactions like Aldol condensation and some fine chemical synthesis.

Acknowledgment. J. A. Wang thanks the CONACyT, Mexico, for the financial support of his postdoctoral study at the Institute of Physics of The National University of Mexico (UNAM), Mexico. We are also grateful to Mr. A. Morales for his technical assistance and to Mrs. R. I. Conde-Velasco for helping in the pyridine FTIR measurements.

References and Notes

(1) Tanabe, T.; Sumiyoshi, T. *New Solid Acid and Bases*, Kodansha: Tokyo, 1989.
(2) Tanabe, T. *Solid Acid and Bases*, Academic Press: New York, 1970.
(3) Ai, M.; Suzuki, S. *J. Catal*. **1972**, *26*, 202.
(4) Ai, M.; Ikawa, T. *J. Catal*. **1975**, *40*, 203.
(5) Gervashi, A.; Auroux, A. *J. Catal*. **1991**, *131*, 190.
(6) Vohs, J. M.; Barteau, M. A. *J. Phys. Chem*. **1991**, *95*, 297.
(7) Larson, S. A.; Widegren, J. A.; Falcner, J. L. *J. Catal*. **1995**, *157*, 611.
(8) Burrows, A.; Kiely, C. J.; Hutchings, G. J.; Joyner, R. W.; Sinev, M. Y. *J. Catal.* **1997**, *167*, 77.
(9) Portillo, R.; López, T.; Gómez, R.; Bokhimi; Morales, A.; Novaro, O. *Langmuir* **1996**, *12*, 40.
(10) Partlow, D. P.; Yoldas, B. E. *J. Non-Cryst. Solids* **1981**, *46*, 153.
(11) Klein, L. C. *Annu. Rev. Mater. Sci*. **1985**, *15*, 227.
(12) Duran, A.; Serna, C.; Fornes, V.; et al. *J. Non-Cryst. Solids* **1986**, *82*, 69.
(13) López, T.; Cruz, G.; Gomez, R. *Mater. Chem. Phys*. **1994**, *36*, 222.
(14) Derouance, E. G.; Fripiat, J. C.; André, J. M. *Chem. Phys. Lett*. **1974**, *28*, 445.
(15) Tsuji, H.; Yagi, F.; Hattori, H.; Kita, H. *J. Catal*. **1994**, *148*, 759.
(16) Zhang, G.; Hattori, H.; Tanabe, K. *Bull. Chem. Soc. Jpn*. **1989**, *62*, 2070.
(17) Bokhimi; Aceves, A.; Novaro, O.; López, T.; Gómez, R. *J. Phys. Chem*. **1995**, *99*, 14403.
(18) Angel, G. D.; Medina, C.; Gómez, R.; Rejai, B.; Gonzalez, R. D. *Catal. Today* **1989**, *5*, 395.
(19) Galvagno, S.; Schwank, J.; Parravano, G. *J. Catal*. **1980**, *69*, 415.
(20) Rhodes, W. H.; Wuensch, B. J. *J. Am. Ceram. Soc*. **1973**, *56*, 495.
(21) Wheat, T. A.; Carruthers, T. G. *Science of Ceramic IV*: Academic Press: London, 1968; p 33.
(22) Eubank, W. R. *J. Am. Ceram. Soc*. **1951**, *34*, 225.
(23) Anderson, P. J.; Horlock, R. F. *Trans. Faraday Soc*. **1962**, *58*, 1993.
(24) Niepce, J. W.; Watelle, G. *J. Phys. Colloq*. **1977**, 365.
(25) Green, I. *J. Mater. Sci*. **1983**, *18*, 637.
(26) Goodman, J. F. *Proc. R. Soc. London* **1958**, *247*, 346.
(27) Kim, M.; Dahmen, G. U.; Searcy, A. W. *J. Am. Ceram. Soc*. **1987**, *70*, 146.
(28) Freund, F.; Spering, V. *Mater. Res. Bull*. **1976**, *11*, 621.
(29) Dasgupta, D. R. *Mineral. Mag*. **1965**, *35*, 623.
(30) Ball, M. C.; Taylor, H. F. W. *Mineral. Mag*. **1961**, *32*, 754.
(31) López, T.; García-Cruz, I.; Gómez, R. *J. Catal*. **1991**, *127*, 75.
(32) Atteta, M.; Klabunde, K. J. *J. Chem. Mater*. **1991**, *3*, 182.
(33) Lin, S.-T.; Klabunde, K. J. *Langmuir* **1985**, *1*, 600.
(34) Li, Y.-X.; Schlup, J. R.; Klabunde, K. J. *Langmuir* **1991**, *7*, 1394.
(35) Li, Y.-X.; Koper, O.; Atteta, M.; Klabunde, K. J. *J. Chem. Mater*. **1992**, *4*, 611.
(36) Zhanpeisov, N. U.; Zhidomirov, G. M.; Yudanov, I. V.; Klabunde, K. J. *J. Phys. Chem*. **1994**, *98*, 10032.
(37) Tobuisune, N.; Hanamaki, C.; Kobayshi, H. *J. Catal.* **1975**, *38*, 101.
(38) Szabo, Z. G.; Jover, B.; Ohmacht, R. *J. Catal*. **1975**, *39*, 225.
(39) Bokhimi, X.; Morales, A.; López, T.; Gómez, R. *J. Solid State Chem*. **1995**, *115*, 411.
(40) Parry, E. P. *J. Catal*. **1963**, *2*, 374.
(41) Wang, J. A.; Novaro, O.; Bohkimi, X.; López, T.; Gómez, R. Manuscript in preparation.